Supplemental Data

Molecular Pharmacology

Hits of a High-Throughput Screen Identify the Hydrophobic Pocket of Autotaxin/Lysophospholipase D as an Inhibitory Surface

James I. Fells, Sue Chin Lee, Yuko Fujiwara, Derek D. Norman, Keng Gat Lim, Ryoko Tsukahara, Jianxiong Liu, Renukadevi Patil, Duane D. Miller, R. Jason Kirby, Sandra Nelson, William Seibel, Ruben Papoian, Abby L. Parrill, Daniel L. Baker, Robert Bittman and Gabor Tigyi

Dept. of Physiology, University of Tennessee Health Science Center, Memphis, TN(JF, SCL, YF, DN, KGL, RT, JL)

Dept. of Pharmaceutical Sciences, University of Tennessee Health Science Center, Memphis, TN (RP, DM)

Drug Discovery Center, University of Cincinnati, Cincinnati, OH,(RK, SN, WS, RP)

Computational Research on Materials Institute, Department of Chemistry, University of Memphis, Memphis, TN(AP, DB)

Department of Chemistry and Biochemistry, Queens College of The City University of New York, Flushing, New York (RB)

Supplemental Figure Legend

Supplemental Figure 1. Characterization of the ATX HTS assay:

Supplemental Figure 2. Activity of ATX mutants. Activity of ATX was assessed by FS-3 assays. Triplicate wells were loaded with 100 ml of reaction cocktail in ATX assay buffer (50 mM Tris, 140 mM NaCl, 5 mM KCl, 1 mM $CaCl_2$, 1 mM $MgCl_2$, pH 8.0), resulting in overall concentrations of 10 mM BSA, 1 mM FS-3, and 0 or 0.5X per well. Ten-fold dilutions of concentrated culture medium from HEK293T transfected with the mutants were added. Fluorescence intensity of FS-3 conversionwas read initially and after 4 hour incubation at 37°C at Ex/Em 485/538 nm. Data are the mean value of the triplicates for each sample and reported as average % activity of ATX compared to the WT ATX sample

Supplemental Figure 3. FS-3 LPC-analog docked into the ATX structure using the MOE software. Note that the hydrocarbon chain analogous to that of LPC occupies the hydrophobic pocket whereas, the fluorochrome is in a space that is distinct from the hydrophobic pocket and distal to the hydrophobic tunnel. This set of interactions makes the FS-3 substrate ideal for identification of both active-site and hydrophobic pocket interacting inhibitors.

Supplemental Figure 1

2 nM ATX incubated for 3 hr appears sufficient for compound screening with S/B > 60, Z' > 0.6, and LPA inhibition near 100%.

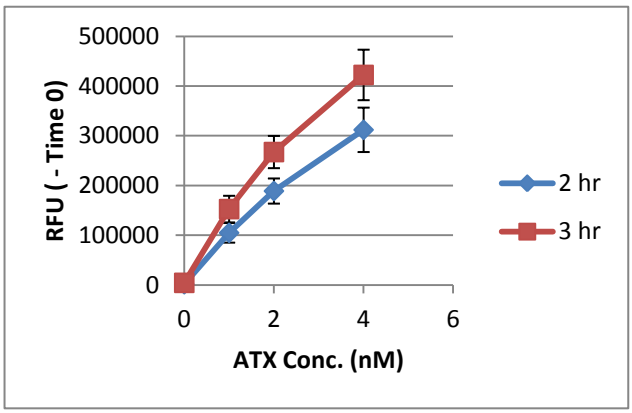

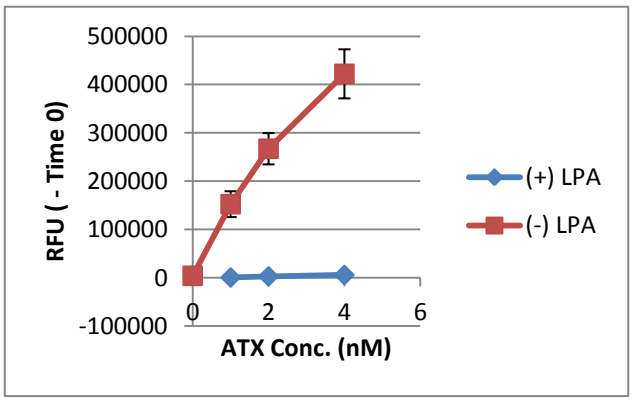

Analysis: Fluorescence data were normalized to the median of neutral controls (2 nM ATX) and inhibitor controls (0 ATX) as follows:

Control	% Activity	
2 nM ATX	0 %	Equivalent to no effect of test compound
0 ATX	-100%	Equivalent to maximum effect of test compound
2 nM ATX + 10 µM LPA	Mean from screen -84.72%	(+) control provides strong inhibition

Results: The assay produced robust results with signal / background (S/B) ratios ranging from 3.14 – 4.70. Results were calculated based on the difference between (-) ATX and (+) ATX at 3 hr. LPA worked very well to inhibit ATX (~ 85%). These plates were repeated a second time with some improvement, but wells that did not produce reliable results were removed from analysis.

% Inhibition	# Compounds	Cumulative # Compounds
90 – 100%	5	5
80 – 90%	19	24
70 – 80%	24	48
60 – 70%	56	104
50 – 60%	94	198
40 - 50%	143	341
30 – 40%	284	625
< 30%	9027	9652

Assay Performance:

	mean	range
S / B	4.19	3.14 – 4.70
Z'	0.847	0.554 – 0.924

Supplemental Figure 2.

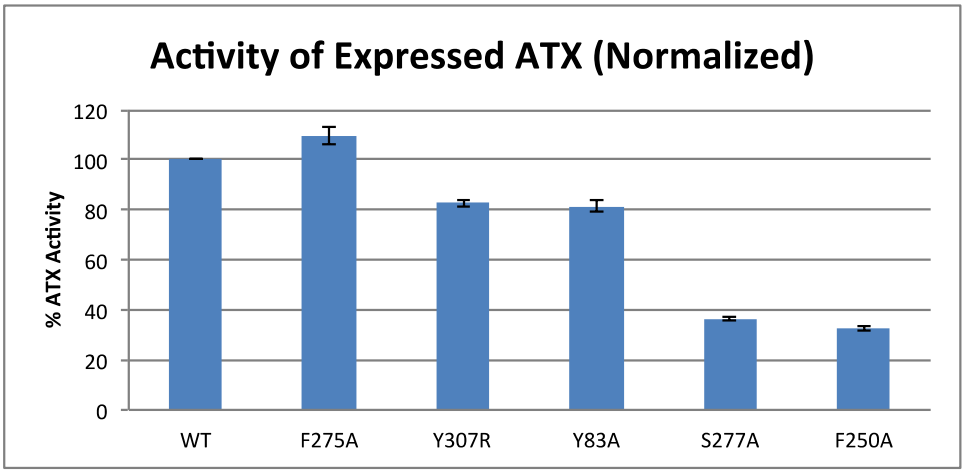

Supplemental Figure 3.

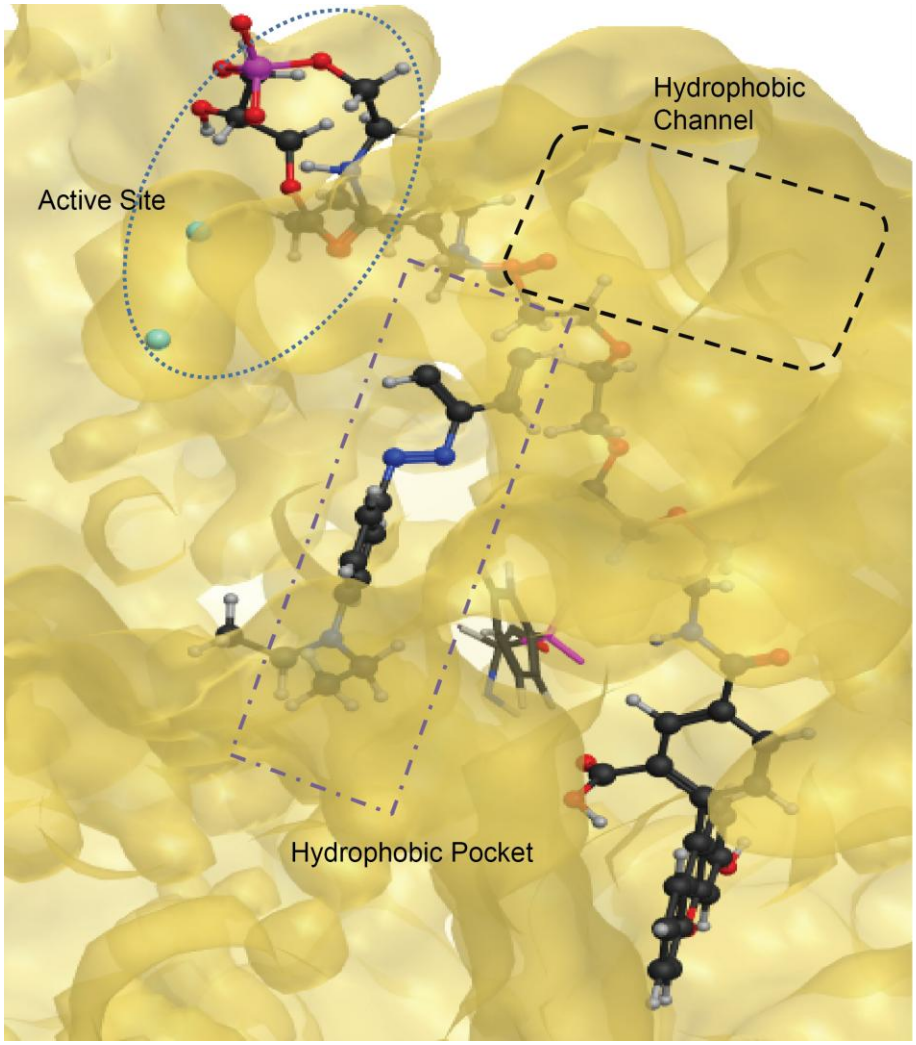

Supplemental Table 1
Inhibitors hits identified by high-throughput screening using FS-3 assay
The structures of the compounds are available from the UC DDC (http://www.drugdiscovery.uc.edu/).

DDC ID	% inhibition
966791	94.52
931126	93.27
918013	91.89
14087	90.43
934399	90.23
946634	88.62
501961	88.34
184018	88.11
766391	87.96
903815	87.57
146638	84.27
994525	84.01
182135	84.01
197620	83.04
182626	82.73
401402	82.52
405628	82.26
587712	82.24
947740	81.7
779181	81.37
923950	80.84
977773	80.42
169992	80.35
942504	80.2
926334	79.04
977533	78.31
929275	77.86
194255	77.53
763068	77.46
504717	77.44
501803	77.3
936332	76.26
129010	75.27
919233	74.93

DDC ID	% inhibition
897131	74.4
800131	74.39
185520	74.33
963604	74.02
923091	73.83
390375	72.89
923745	72.78
944059	72.74
195845	72.61
773518	71.69
396852	71.6
155248	70.96
150748	70.64
934962	70
189581	69.93
928551	69.78
990364	69.06
793165	68.75
171842	68.33
911161	67.93
856398	67.87
185153	67.77
924414	67.7
236689	67.65
194992	67.63
503843	67.56
929372	67.04
492324	66.89
182507	66.63
897143	66.61
396446	66.45
714508	66.37
989814	65.98
501385	65.94

DDC ID	% inhibition
979420	65.81
411727	65.33
977136	64.28
383926	63.87
1007456	63.74
965199	63.69
1007714	63.3
98870	63.27
946284	63.23
949538	62.97
913315	62.68
726654	62.39
152382	62.32
1003272	62.31
379917	62.28
185505	62.24
966139	61.99
373724	61.73
94289	61.67
764694	61.61
774500	61.51
405726	61.37
386011	61.25
918217	61.1
966800	61.08
925321	60.85
249643	60.84
938976	60.7
118865	60.5
990571	60.4
194279	60.37
994461	60.3
924266	60.25
920540	60.1

MOL #87080

DDC ID	% inhibition
226845	60.03
13663	60.01
171358	59.96
923027	59.95
153053	59.39
502095	59.36
262052	59.33
253051	59.16
503583	59.04
937347	58.96
773563	58.79
930769	58.76
766346	58.55
194780	58.42
902881	58.37
945497	58.27
912368	58.18
947144	58.04
253862	57.97
935401	57.93
197127	57.7
149849	57.66
188616	57.22
291732	56.8
119479	56.79
916694	56.78
182831	56.72
521161	56.29
382296	56.28
181493	56.26
787625	55.95
946793	55.83
193595	55.78
702352	55.76
114199	55.57
966240	55.52
901656	55.37
543450	55.13
928933	55.12

DDC ID	% inhibition
503380	54.98
798171	54.75
928943	54.62
232620	54.48
518182	54.47
1009104	54.37
994194	54.36
519793	54.25
406557	54.14
1002382	54.09
128624	54.07
518033	53.93
787517	53.9
757999	53.89
989985	53.74
254179	53.57
967605	53.5
764910	53.5
953225	53.4
9896	53.38
263156	53.29
945159	53.19
963522	53.02
860716	52.95
892478	52.88
990463	52.82
291709	52.82
383544	52.6
391849	52.45
543599	52.41
194072	52.4
944610	52.33
251599	52.17
761498	52.03
123162	51.85
825594	51.81
511135	51.79
995092	51.63
934493	51.51

DDC ID	% inhibition
186010	51.45
389078	51.41
193649	51.28
966949	50.99
414096	50.98
994691	50.81
949724	50.8
954432	50.73
919079	50.49
952461	50.46
527595	50.46
929785	50.44
936588	50.34
977219	50.33
251643	50.33
1009281	50.31
934313	50.31
251606	50.2

Supplemental Table 2.

Reported IC_{50} values identified in the original high-throughput screen.

DDC ID	IC50(nM)
903815	4.29
931126	6.50
918013	31.42
966791	53.05
406643	54.32
897903	59.93
501961	61.47
182135	153.50
390596	170.40
503380	209.50
898736	233.20
923091	235.50
783342	241.00
408829	289.60
947740	380.80
946793	386.40
977773	421.90
781579	435.10
504717	500.50
918217	546.80
501803	646.60
918217	789.30
856398	816.00
527279	854.70
942504	888.90
937459	954.90